Title: In situ microscope FTIR studies of methanol adsorption and oxidation on an individually addressable array of nanostructured Pt microelectrodes

Authors: Jun-Tao Li, Qing-Song Chen, Shi-Gang Sun

PII: S0013-4686(07)00067-9
DOI: doi:10.1016/j.electacta.2006.12.082
Reference: EA 12243

To appear in: *Electrochimica Acta*

Received date: 5-10-2006
Revised date: 17-12-2006
Accepted date: 17-12-2006

Please cite this article as: J.-T., Li, Q.-S., Chen, S.-G., Sun, In situ microscope FTIR studies of methanol adsorption and oxidation on an individually addressable array of nanostructured Pt microelectrodes, *Electrochimica Acta* (2007), doi:10.1016/j.electacta.2006.12.082

In situ microscope FTIR studies of methanol adsorption and oxidation on an individually addressable array of nanostructured Pt microelectrodes

Jun-Tao Li, Qing-Song Chen and Shi-Gang Sun*

State Key Laboratory of Physical Chemistry of Solid Surfaces, Department of Chemistry, College of Chemistry and Chemical Engineering, Xiamen University, Xiamen 361005, China

Abstract An individually addressable array of nanostructured Pt microelectrodes was designed and prepared according to the concept of combinatorial electrochemistry. Different nanostructures on the array were obtained systematically by electrochemical deposition under cyclic voltammetric conditions. The surface structure and electrochemical behavior of the array were investigated respectively using scanning tunneling microscopy (STM) and cyclic voltammetry (CV), and electrocatalytic properties of the array towards methanol oxidation were studied by CV and in situ microscope Fourier transform infrared reflection spectroscopy (MFTIRS). The results revealed the higher electrocatalytic activity of nanostructured Pt surfaces, and demonstrated that the combination of an individually addressable array with in situ MFTIRS is an efficient combinatorial approach in studies of electrocatalytic reaction processes at molecular level.

Keywords: Methanol oxidation, individually addressable array, nanostructured Pt microelectrodes, in situ MFTIRS, combinatorial approach

1. Introduction

The direct methanol fuel cell (DMFC) is known as one of the most promising power sources for transportation vehicles and portable electronic devices, thanks to its

* ISE member and correspondence author, Fax: +86 592 2183047, Email: sgsun@xmu.edu.cn

high energy density, ease in the handling of liquid fuel, and low operating temperature. The electrocatalysis of methanol oxidation is the key issue of DMFC, because Pt-based anodic catalysts suffer frequently from the self-poisoning phenomenon that is caused by poisoning intermediates (mostly CO species) derived from dissociative adsorption of methanol on catalyst surface. Considerable efforts have been devoted to investigate the mechanism of methanol electrooxidation and to prepare catalysts of superb properties including high tolerance for poisoning and high activity to methanol oxidation [1-3]. Extensive studies demonstrated that the properties of Pt-based electrocatalysts depend strongly on their chemical composition, surface atomic arrangement and electronic structure, etc. Thus it may be a tough task to screen out the best electrocatalyst among so many parameters. The conventional electrochemical method is time-consuming when it is used to characterize the properties of electrocatalyst through a try and error strategy. In addition the study is even complicated by the variety of components and structures of individual electrocatalyst. Combinatorial methods, based on the principle of parallelism, enable preparing library of large amount of catalysts and evaluating their property in a short time. The key issue for the successful application of combinatorial analysis is to set up a proper method for screening sample library. Since the pioneer work of Smotkin's group in combinatorial screening of multi-component electrocatalysts towards methanol electrooxidation [4], different combinatorial electrochemical methods based on electrode arrays and parallel detection have been developed [5-10]. Hayden et al. have reported recently both Pt-based alloy composition [11] and Au particle size [12] dependences of electrocatalysts through the use of a large (10x10) array in electro-combinatorial studies. All previous electro-combinatorial studies were focused on screening the composition and structure of electrocatalysts for diverse applications. To our knowledge, no attention has been paid so far to investigate electrocatalytic reaction processes on different electrocatalysts at molecule level under combinatorial consideration. We have recently developed an approach of combinatorial spectroelectrochemical analysis through combining in situ microscope FTIR spectroscopy (MFTIRS) with an individually addressable array of microelectrodes

[13]. This method was applied successfully in investigation of the anomalous IR properties of nanostructured film materials of Pt [14], Ru [15] and Pd [16]. The emphasis has been put on the structure, the particle size and the IR optical properties. Umeda et al. demonstrated furthermore that microelectrode is an efficient device for studying electrode reaction of DMFC [17, 18]. In this paper we designed and prepared an individual array of Pt microelectrodes with different nanostructures. Through the combination of the array with in situ MFTIRS, electrocatalytic reaction of methanol on the array was studied. The study has thrown new insight into combinatorial analysis of methanol oxidation on nanostructured Pt electrocatalysts at molecule level.

2. Experimental

2.1 Preparation of individually addressable array of Pt microelectrodes with different nanostructures.

Nine Pt wires of 200 μm in diameter were hosted orderly in a Teflon template that ensures the arrangement of 9 Pt microelectrodes (PtMEs) as a 3×3 matrix (Fig. 1). The center-to-center distance between neighboring microelectrodes was fixed at 1.0 mm. In such an arrangement coupling effects between the PtMEs could be avoided. A homemade switch box was designed to connect any individual or a group of the PtMEs to potentiostat. Electrodeposition was carried out in 2 mM K_2PtCl_6 + 0.1 M $HClO_4$ solution under cyclic voltammetry (CV) conditions, in which the lower and upper limits of potential scan were set at -0.25 and 0.35 V, respectively. The structures of Pt thin films on the array were controlled by varying the number of potential cycle, *n*, from 0 to 160 with an interval of 20. The PtME that was prepared with electrodeposition of *n* cycles was denoted as PtME(*n*) thereafter. After the preparation, the array was transferred to another cell containing 0.5 M H_2SO_4 solution, and subjected to a pre-treatment of cyclic potential scans between -0.25 and 1.25 V at a scan rate 0.10 $V \cdot s^{-1}$ to clean the electrode surface until stable cyclic voltammograms (CVs) were recorded.

2.2 In situ microscope FITR spectroscopy (in situ MFTIRS)

In situ MFTIRS was described in detail elsewhere [13]. In brief, it consists of mainly a Nexus 870 FTIR spectrometer (Nicolet), a microscope (IR-Plan® Advantage , Spectra-Tech Inc.) equipped with a narrow-range HgCdTe detector (MCTA, with the HgCdTe photodiode size of 250 μm × 250 μm) cooled with liquid N_2, and a thin-layer IR cell working with the array of Pt microelectrodes. A motorized X-Y stage was employed to position readily each microelectrode of the array on the focusing point of IR microscope. A CaF_2 disk was used as IR window, and the thin layer of solution was formed by moving the array against the IR window during in situ MFTIRS measurements. Single potential alternation FTIR (SPAFTIR) [19] procedure was used in this study to investigate methanol oxidation. Before this procedure, the electrode potential was stayed at 1.20 V for 5 s to clean the surface of PtME(*n*) and remove any adsorbates by oxidation, then switched to -0.20 V and remained for 2 min to refresh the thin layer of solution. The reference single-beam spectrum $R(E_R)$ and sample single-beam spectrum $R(E_S)$ were collected at reference potential E_R and sample potential E_S, respectively. The resulting spectrum was calculated by Eq (1).

$$\frac{\Delta R}{R}(E_S) = \frac{R(E_S) - R(E_R)}{R(E_R)} \qquad (1)$$

The mutlistep FTIR (MSFTIR) procedure [20] was also used in this study to investigate IR properties of the array employing CO adsorption as probe reaction. In this procedure a series of $R(E_S)$ were collected firstly at E_S, where adsorbed CO (CO_{ad}) is stable on electrode surface, then $R(E_R)$ was collected at E_R, at which CO_{ad} has been removed completely by electrooxidation. The resulting spectrum was also calculated using Eq.(1).

Each single-beam spectrum was acquired by collecting and coadding 100 interferograms at a spectral resolution of 8 cm^{-1}.

2.3 Other conditions

A 263 potentiostat/galvanostat (EG&G) was used to control electrode potential in this study. The characterization of surface structures of the PtME(*n*) was carried out on a P4-18-SPM scanning tunneling microscope (STM) (NT-MDT). The reference

electrodes used in both electrochemical experiments and in situ MFTIRS studies were a standard saturated calomel electrode (SCE) and a Pd wire saturated with hydrogen (Pd|H), respectively. To the facility of discussion, however, all potentials presented in this paper were quoted versus the SCE scale. Solutions were prepared from superpure H_2SO_4 and Millipore water supplied from a Milli-Q lab equipment (Nihon Millipore Ltd.). The solutions were deaerated by purging with pure N_2 gas before experiment and a flux of N_2 was kept flowing over the solution during measurements to prevent interference of atmospheric oxygen. All experiments were carried out at room temperature.

3 . Results and Discussion

3.1 STM studies

Fig.2 shows STM images of 4 typical PtME (n=40, 80, 120, 160) on the array. We can observe that nanostructures consisted of island-shaped Pt crystallites were formed on the array in cyclic voltammetric electrodeposition. Continuous electrodeposition with n increasing leads to increase gradually the average size of Pt islands and the average thickness of the nanostructured films of PtME(n). The average size of Pt islands in Fig.2 was measured respectively about 141 nm for PtME(40), 161 nm for PtME(80), 197 nm for PtME(120) and 247 nm for PtME(160).

3.2 CV studies

Fig.3 illustrates the comparison of cyclic voltammograms (CVs) of PtME(n) on the array recorded in 0.5 M H_2SO_4 at scan rate 0.1 $V \cdot s^{-1}$. Well-defined CVs features of a Pt polycrystalline electrode are observed on all PtMEs. That is, (1) two pairs of current peaks appear around -0.13 V and 0.02 V due to hydrogen adsorption/desorption. The pair of current peaks at around -0.13 V can be ascribed to hydrogen adsorption/desorption on surface (111) or (110) sites of Pt, and that near 0.02 V could be attributed to hydrogen adsorption/desorption on surface (100) sites of Pt; (2) two anodic current peaks at 0.74 and 0.81 V and a current plateau at more positive potentials occur in the positive-going potential scan (PGPS). In the

negative-going potential scan (NGPS), a cathodic peak near 0.48 V is observed. These features have been assigned to electroformation and electroreduction of an oxygen-containing layer on the PtME surface. It is clear that the current in CVs gradually increases from PtME(0) to PtME(160). The electric charge of hydrogen adsorption (Q_H^n) measured by integration of the CV curve can be used to evaluate quantitatively the electrochemical active surface area of the PtME(n) [21, 22]. Since all PtMEs on the array hold the same geometric area of 3.14×10^{-4} cm^2, the relative surface roughness of the PtME(n) (R_H^n) can also be therefore definded by comparing the charge of hydrogen adsorption integrated from CVs according to Eq. (2), i.e. the ratio of the Q_H^n acquired on PtME(n) to the Q_H^0 measured on PtME(0). It can be seen from Fig.4 that the R_H^n is increased linearly from PtME(0) to PtME(160), with a maximal value of 68.0 on PtME(160).

$$R_H^n = \frac{Q_H^n}{Q_H^0} \tag{2}$$

Fig.5 displays the CVs of PtME(140) in 0.1 M CH_3OH + 0.5 M H_2SO_4, at scan rate 0.005 $V\cdot s^{-1}$. In the PGPS, the onset potential of methanol oxidation was observed at about 0.15 V, at which poisoning CO-type species can be removed by reaction with electroadsorbed OH species derived from water dissociation [23, 24]; methanol oxidation yields then a current peak at 0.557 V; further increase of potential methanol oxidation is inhibited by Pt oxide formation on electrode surface. In the NGPS, methanol oxidation restarts at the potential where the Pt oxide is partially reduced, then gives rise to a current peak at 0.486 V. Similar CV features are observed on other PtME(n). The peak current I_P and peak potential E_P measured from the CVs of methanol oxidation on PtME(n) in PGPS are listed in Table 1. We can see that the I_P increased linearly from 0.158 μA on PtME(0) to a maximal value 12.54 μA on PtME(160). It is interesting to observe that the E_P on nanostructured PtMEs is always shifted negatively in comparison with the value measured on the PtME(0), illustrating the higher activity of the nanostructured PtMEs than that of the bulk PtME for methanol oxidation.

3.3 In situ MFTIRS studies

The characterization of methanol oxidation by CV can not readily provide clear indications of the nature of intermediates and oxidation products. We have used therefore in situ MFTIRS technique to investigate further the oxidation process of methanol on PtME(*n*) at molecule level. For a conventional electrode employed in normal IR spectroscopy, i.e a disk electrode of a few mm in diameter, the thin layer between the IR window and electrode in the IR cell has to be refreshed after each SPAFTIR experiment because of the vast consumption of reagent in reaction. Thanks to advantages of microelectrode in terms of fast mass transport, rapid respondance to potential alteration and less consumption of reagent, it is not necessary to refresh the thin layer after each SPAFTIR measurement for studies of irreversible electrocatalytic reactions. As a consequence, the experiment with microelectrode and in situ microscope FTIRS presents an advantage in terms of time saving. Moreover, surface structure of the PtME(*n*) can be avoided from demolishing by frequently adjusting the thin layer and the electrode position to IR incident beam during study of methanol oxidation in studies by using MFTIRS.

3.3.1 Typical IR features of methanol adsorption and oxidation on the PtME(n)

In order to present clearly IR results of menthol oxidation on the array, the data obtained on PtME(140) are discussed firstly. SPAFTIR spectra of methanol adsorption and oxidation on PtME(140) in 0.1 M CH_3OH + 0.5 M H_2SO_4 are displayed in Fig.6, with the reference spectrum collected at -0.20 V. When $E_S \geq 0.2$V, significant IR bands appear in spectra associating with methanol oxidation, which can be correlated with the CVs data in Fig.5. Accompanying with adsorption and oxidation of methanol in the thin layer, positive bands are observed around 2950, 2842 and 1014 cm^{-1}, which are attributed to the loss of methanol. A positive band near 1641 cm^{-1} and a negative band at 2345 cm^{-1} are assigned respectively to the consumption of H_2O and the production of CO_2. A bipolar band is appeared approximately at 2050 cm^{-1}, corresponding to the adsorption of linearly bonded CO

species (CO_L) that are derived, on the one hand, from dissociative adsorption of methanol on the PtME(140), and are generated in methanol oxidation, on the other hand. So the adsorbed CO species may be ascribed to intermediates involved in methanol oxidation. The details of the CO_L band are illustrated clearly in Fig.8a and will be discussed below.

The variations of the intensity of CO_2 band I_{CO2} and that of CO_L band I_{COL} with Es on PtME(140) are plotted in Fig. 7. A slow growth of I_{CO2} from 0.00 to 0.20 V, and a rapid increase form 0.20 to 0.46 V are observed. A maximum value is appeared at 0.46 V, after which I_{CO2} decays because of the diffusion of CO_2. The I_{COL} increased from 0.00 to 0.30 V and reaches its maximum value at 0.30 V, after which it decays due to the oxidation of CO. It is interesting to note that the shape of bipolar CO_L band derived from methanol is potential dependent (see Fig. 8a). From 0.00 to 0.25V, the upward peak of the bipolar band locates at higher wavenumber, however, when E_S is above 0.30 V, the upward peak is at lower wavenumber referring to the downward peak, while the CO_L at 0.3 V is likely a distorted monopolar band. Fig 8b gives the MSFTIR spectra of pre-saturation adsorption of CO on PtME(140) form -0.20 V to 0.30 V by setting the E_R at 0.80 V, where the CO is removed completely by electrooxidation. As a consequence, the MSFTIR spectra illustrate the intrinsic IR properties of CO adsorbed on PtME(140). It can be seen that the IR band of pre-saturated CO_L on PtME(140) yields a bipolar band whose upward peak lies in higher wavenumber than that of its downward peak. It is known that such bipolar IR features are typical characteristics of the Fano-like spectral line shape [25-27]. When $E_S \geq$ 0.25V, the intensity of CO_L band decreases progressively due to CO oxidation. The shape of pre-saturated CO_L band , however, does not change with E_S. So we can explain the change in shape of the IR band of CO_L species derived from methanol with E_S on PtME(140) (see Fig.8a) as following. Methanol can be dissociatively adsorbed on electrode at -0.2 V, where $R(E_R)$ is collected. When E_S is increased form 0.00 to 0.25 V, the intensity of upward and downward peaks of the bipolar band increase, the resulting spectra that are according to Eq.(1) give rise to a bipolar band with the upward peak lying in higher wavenumber. When the E_S is increased continuingly, CO_L derived form methanol is oxidized and the $R(E_S)$ collected at E_S does not contain IR adsorption CO_L species. After the calculation by using Eq.(1), the resulting spectra are IR absorption of the CO_L species derived from methanol at -0.2 V,

and are illustrated as inverted bipolar band.

When E_S becomes move positive than 0.3 V, small negative bands near 1338 and 1099 cm^{-1} can be attributed to IR adsorption of -COOH group, which suggests the active intermediate of the methanol oxidation may contain -COOH group. The negative bands near 1193 and 1054 cm^{-1} are originated from IR absorption of an enhanced interfacial HSO_4^-/HSO_4^{2-} concentration due to the increase of H^+ in the oxidation of methanol.

3.3.2 IR spectral features of methanol adsorption and oxidation on PtME(n)

It is known that before their oxidation, the CO_{ad} species derived from methanol may act as poison to inhibit the electrooxidation of methanol. It is also reported that the formation of CO from methanol dissociative adsorption is structure sensitive [28]. So, it is necessary to analyze in detail the IR features of CO_L species derived from methanol on PtME(*n*) in low potential region. Fig.9 shows the comparison of IR spectra of the CO_L derived form methanol (Fig.9a) and the pre-saturated CO_L (Fig. 9b) on PtME(*n*) of the array at 0.20 V. As shown in Fig.9b, on the PtME(0), i.e. the bulk Pt microelectrode, the pre-saturated CO_L yields a normal IR absorption band appearing in a negative-going direction. The pre-saturated CO_L on the PtME(*n*) with *n* increasing from 20 to 160 gives rise always to a bipolar band, i.e. the Fano-like spectral line shape. The IR bands of the CO_L species derived from methanol on nanostructured PtME(*n*) are also bipolar at 0.20 V, whose shape does not change regularly with *n*. The intensity of the CO_L band derived from methanol, however, increases almost linearly with the increase of *n* from PtME(0) to PtME(160), as listed in table 2. This result suggests that the dissociative adsorption of methanol on Pt surface is structure sensitive, and has demonstrated that the increase of surface roughness is helpful for IR determination of adsorbed species on the surface of electrode.

Fig.10 compares the SPAFTIR spectra of methanol oxidation on different nanostructured PtMEs on the array at 0.40 V, at which methanol can be oxidized completely as illustrated previously. CO_2 band at 2345 cm^{-1}, CH_3OH band at 2950, 2842, 1014 cm^{-1}, -COOH group band at 1338, 1099 cm^{-1}, H_2O band at 1064 cm^{-1} and

HSO_4^- band at 1193, 1054 cm^{-1} are observed in spectra acquired on all nanostructured PtME(*n*). The intensity of above bands is varied irregularly with the increase of *n* (see Fig.11). As we know that all above species exist in the thin layer between IR window and microelectrode, the diffusion of these species is then a main issue to affect the intensity of these IR bands, when the concentration of these species is varied along with methanol oxidation. This phenomenon is especially distinct when electrode is at micro-scale. Thus in the case of combinatorial SPAFTIR experiments with microelectrodes, the quantitative detection of solution species such as CO_2 in the thin layer between the IR window and microelectrode is not as precise as the detection of the species adsorbed on microelectrode such as CO, due to the diffusion during IR data collection.

4. Conclusions

The current study has put emphasis upon a combinatorial approach of investigation of methanol oxidation on nanostructured Pt electrocatalysts at molecule level. It has also expanded the application of microelectrode array in electrocatalysis.

STM studies demonstrated that island-shaped Pt crystallites were formed on Pt microelectrode substrate in cyclic voltammetric deposition. The average size of the Pt islands and the average thickness of nanostructured Pt films were increased with increasing the electrodeposition cycles (*n*). Cyclic voltammetry studies illustrated that the current peak I_P of methanol oxidation is increased linearly with *n,* and the peak potential E_P is shifted negatively referring to that on a bulk PtME, suggesting that nanostructured PtME(*n*) on the array is more active than the PtME(0), i.e. bulk Pt, for methanol oxidation.

In situ MFTIRS has determined on PtME(*n*) of the array, just like on a conventional Pt electrode, CO_2, CO, -COOH, H_2O and HSO_4^- species involved in methanol adsorption and oxidation. The intensity of linearly adsorbed CO species derived from methanol is increased almost linearly with *n*, while the intensity of solution species in thin layer between IR window and microelectrode is changed irregularly with *n* due to the diffusion of these species. The results indicate that in case of combinatorial analysis using in situ SPAFTIR procedure together with

microelectrode, the quantitative detection of solution species is not as precise as the detection of adsorbed species on microelectrode. Thus, in this combinatorial approach, IR band intensity of adsorbed species is suitable for quantitative comparison, while the IR band intensity of solution species in the thin layer is only appropriated for qualitative analyses. In situ MFTIRS studies have revealed further that the adsorbed CO on these nanostructured PtMEs yields a Fano-like spectra, while the adsorbed CO on bulk PtME gives rise to a normal spectrum.

This study demonstrated that the combination of an individually addressable array of Pt microelectrodes with in situ MFTIRS is a promising combinatorial means for the investigation of electrocatalytic reaction processes at molecule level.

Acknowledgements

The studies were supported by NSFC (20373059, 20433060, 20673091) and subsidized by the Special Funds for Major State Basic Research Project of China (2002CB211804).

References

[1]. S. Wasmus, A. Kuver, J. Electroanal. Chem. 461 (1999) 14.

[2]. J. Kua, W. A. Goddard, J. Am. Chem. Soc. 121 (1999) 10928.

[3]. T. Iwasita, Electrochim. Acta 47 (2002) 3663.

[4]. E. Reddington, A. Sapienza, B. Gurau, R. Viswanathan, S. Sarangapani, E.S. Smotkin, T.E. Mallouk, Science 280 (1998) 1735.

[5]. J.L. Fernandez, D.A. Walsh, A.J. Bard, J. Am. Chem. Soc. 127 (2005) 357.

[6]. R.Z. Jiang, C. Rong, D. Chu, J. Comb. Chem. 7 (2005) 272.

[7]. S. Guerin, B.E. Hayden, C.E. Lee, C. Mormiche, J.R. Owen, A.E. Russell, B. Theobald, D. Thompsett, J. Comb. Chem. 6 (2004) 149.

[8]. M.D. Fleischauer, T.D. Hatchard, G.P. Rockwell, J.M. Topple, S. Trussler, S.K. Jericho, M.H. Jericho, J.R. Dahn, J. Electrochem. Soc. 150 (2003) A1465.

[9]. P. Strasser, Q. Fan, M. Devenney, W.H. Weinberg, P. Liu, J.K. Norskov, J. Phys. Chem. B 107 (2003) 11013.

[10]. W.C. Choi, J.D. Kim, S.I. Woo, Catal. Today 74 (2002) 235.

[11]. S.Guerin, B.E. Hayden, C.E. Lee, C. Mormiche, A.E. Russell, J. Phys. Chem. B 110 (2006) 14355.

[12]. S. Guerin, B.E. Hayden, D. Pletcher, M.E. Rendall, J.-P. Suchsland, J. Comb. Chem. 8 (2006) 679.

[13]. H. Gong, S.G. Sun, Y.J. Chen, S.P. Chen. J. Phys. Chem. B 108 (2004) 11575.

[14]. Y.J. Chen, S.G. Sun, S.P. Chen, J.T. Li, H. Gong, Langmuir 20 (2004) 9920.

[15]. H. Gong, S.G. Sun, J.T. Li, Y.J. Chen, S.P. Chen, Electrochim. Acta 48 (2003) 2933.

[16]. J.T. Li, Y.J. Chen, Z.F. Su, Z.Y. Zou, S.P. Chen, S.G. Sun, Chem. J. Chinese Univ. 26 (2005) 710.

[17]. M. Umeda, M. Mohamedi, I. Uchida, Langmuir 17 (2001) 7970.

[18]. M.Umeda, M. Kokubo, M. Mohamedi, I. Uchida, Electrochim. Acta 48 (2003) 1367.

[19]. D.S. Corrigan, L.W.H. Leung, M.J. Weaver, Anal. Chem. 59 (1987) 2252.

[20]. W.F. Lin, S.G. Sun, Electrochim. Acta 41 (1996) 803.

[21]. M. Watanabe, K. Makita, H. Usami, S. Motoo, J. Electroanal. Chem. 197 (1986) 195.

[22]. G. Faubert, D. Guay, J.P. Dodelet, J. Electrochem. Soc. 145 (1998) 2985.

[23]. J. Willsau, J. Heitbaum, Electrochim. Acta 31 (1986) 943.

[24]. P. Waszczuk, A.Wieckowski, P. Zelenay, S. Gottesfeld, C. Coutanceau, J.M. Leger, C. Lamy, J. Electroanal. Chem. 511 (2001) 55.

[25]. U. Fano, Phys. Rev. 124 (1961) 1866.

[26]. Y. Zhu, H. Uchida, M. Watanabe, Langmuir 15 (1999) 8757.

[27]. A. Priebe, M. Sinther, G. Fahsold, A. Pucci, J. Chem. Phys. 119 (2003) 4887.

[28]. X.H. Xia, T. Iwasita, F. Ge, W. Vielstich, Electrochim. Acta 41 (1996) 711.

Legend of Figures and Tables

Fig. 1. Individually addressable array of Pt microelectrodes.

Fig. 2. 2-dimensional STM images of: (a) PtME(40), (b) PtME(80), (c) PtME(120) and (d) PtME(160). I_t = 0.200 nA, V_b = 0.150 V.

Fig. 3. CVs of PtME(n) on the array in 0.5 M H_2SO_4 solution, sweep rate 0.10 V·s^{-1}.

Fig. 4. Variations of Q_H^n and R_H^n on PtME(n) with n.

Fig. 5. CVs of methanol oxidation on PtME(140) in 0.1 M CH_3OH + 0.5 M H_2SO_4 solution, sweep rate 0.005 V·s^{-1}.

Fig. 6. In situ SPAFTIR spectra form methanol oxidation on PtME(140) in 0.1 M CH_3OH + 0.5 M H_2SO_4 solution, E_R = -0.20 V, E_S values are indicated in the spectra.

Fig. 7. Variation of I_{COL} and I_{CO2} with E_S, which obtained from the SPAFTIR spectra of methanol oxidation on PtME(140) in 0.1 M CH_3OH + 0.5 M H_2SO_4 solution.

Fig. 8. (a) In situ SPAFTIR spectra of CO_L derived from CH_3OH on PtME(140) in 0.1 M CH_3OH + 0.5 M H_2SO_4 solution, E_R = -0.20 V. (b) In situ MSFTIR spectra of pre-saturated CO adsorbed on PtME(140) in 0.50 M H_2SO_4 solution saturated with CO, E_R= 0.80 V.

Fig. 9. (a) In situ SPAFTIR spectra of CO_L derived from CH_3OH on PtME(n) in 0.1 M CH_3OH + 0.5 M H_2SO_4 solution. E_S = 0.20 V, E_R = -0.20 V. (b) In situ MSFTIR spectra for pre-saturated CO adsorbed on PtME(n) in 0.50 M H_2SO_4 saturated with CO. E_S = 0.2V, E_R = 0.80 V.

Fig. 10. In situ SPAFTIR spectra of methanol oxidation on PtME(n) in 0.1 M CH_3OH + 0.5 M H_2SO_4 solution, E_R = -0.20 V, E_S=0.4V.

Fig. 11. Comparison of the intensity of CH_3OH band at 2842 cm^{-1}, CO_2 band at 2345 cm^{-1} and HSO_4^{1-} band at 1193 cm^{-1} on PtME(n) at 0.40 V, obtained from the SPAFTIR spectra of methanol oxidation in 0.5 M H_2SO_4 + 0.1 M CH_3OH solution, E_R = -0.20 V.

Table 1. Comparison of E_p and I_p of the CVs on the PtME(n) in 0.1 MCH_3OH + 0.5 M H_2SO_4 solution, sweep rate 0.005 V·s^{-1}.

Table 2. List of I_{COL} derived methanol on PtME(n) at 0.20 V, which obtained from SPAFTIR spectra of methanol oxidation in 0.1 M CH_3OH + 0.5 M H_2SO_4 solution , E_R = -0.20 V.

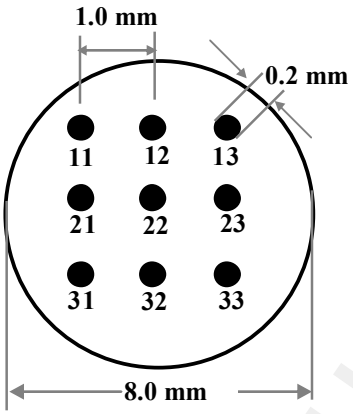

Fig. 1 Illustration of an individually addressable array of Pt microelectrodes.

Li, J. T.; Sun, S. G. et al., Fig.1

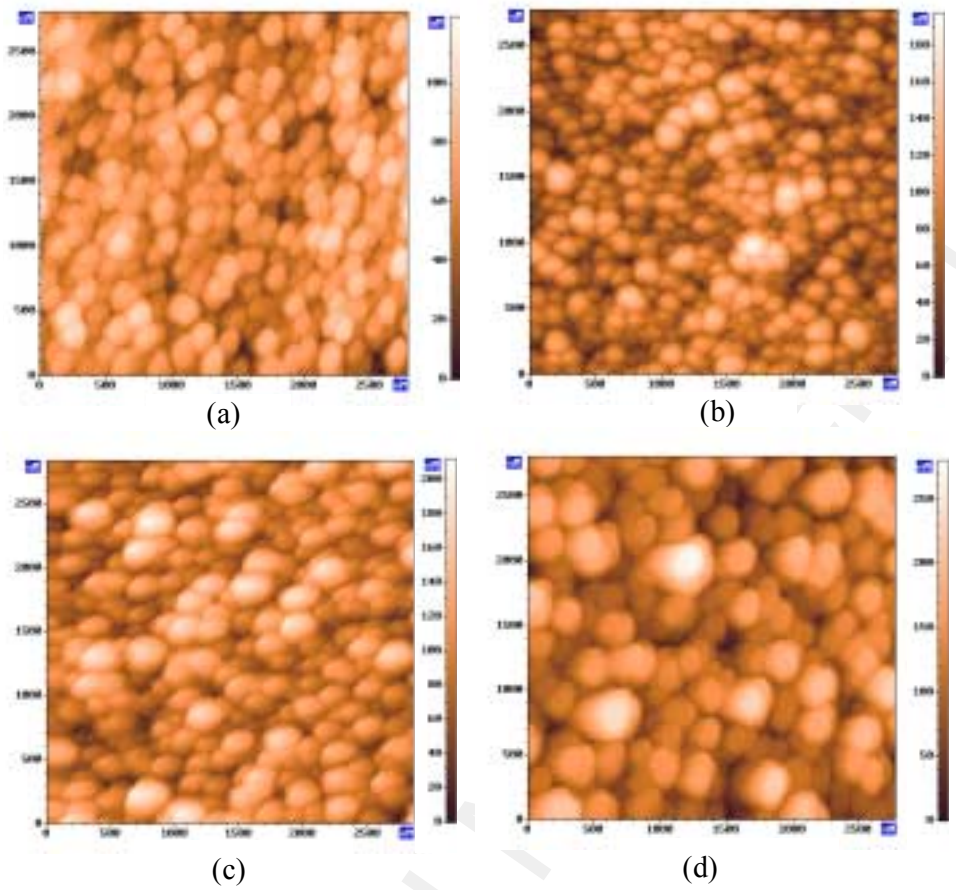

Fig. 2 2-dimensional STM images of: (a) PtME(40), (b) PtME(80), (c) PtME(120) and (d) PtME(160). I_t = 0.200 nA, V_b = 0.150 V.

Li, J. T.; Sun, S. G. et al., Fig. 2

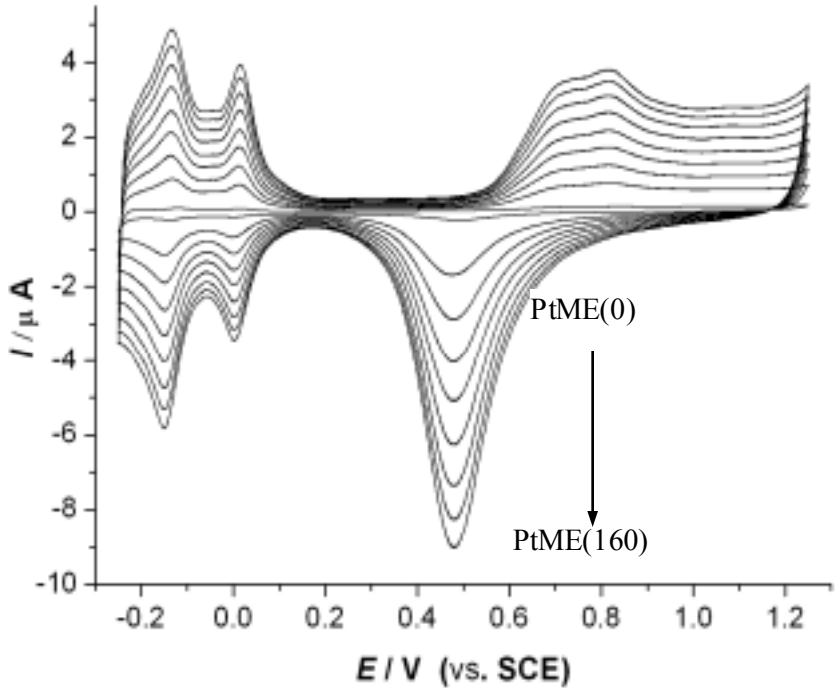

Fig. 3 CVs of PtME(*n*) on the array in 0.5 M H_2SO_4 solution, sweep rate 0.10 $V \cdot s^{-1}$.

Li, J. T.; Sun, S. G. et al., Fig. 3

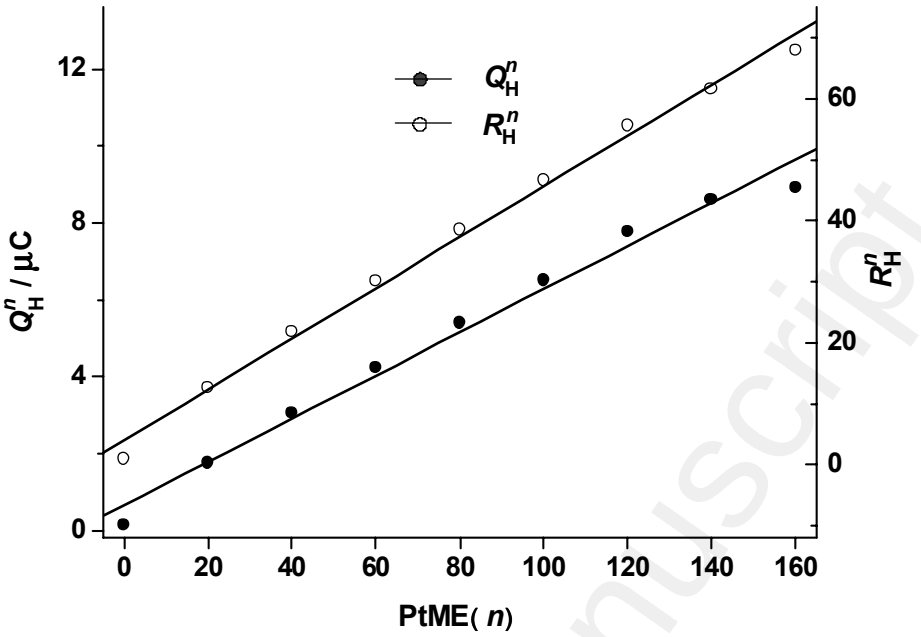

Fig. 4 Variations of Q_H^n and R_H^n with n

Li, J. T.; Sun, S. G. et al., Fig. 4

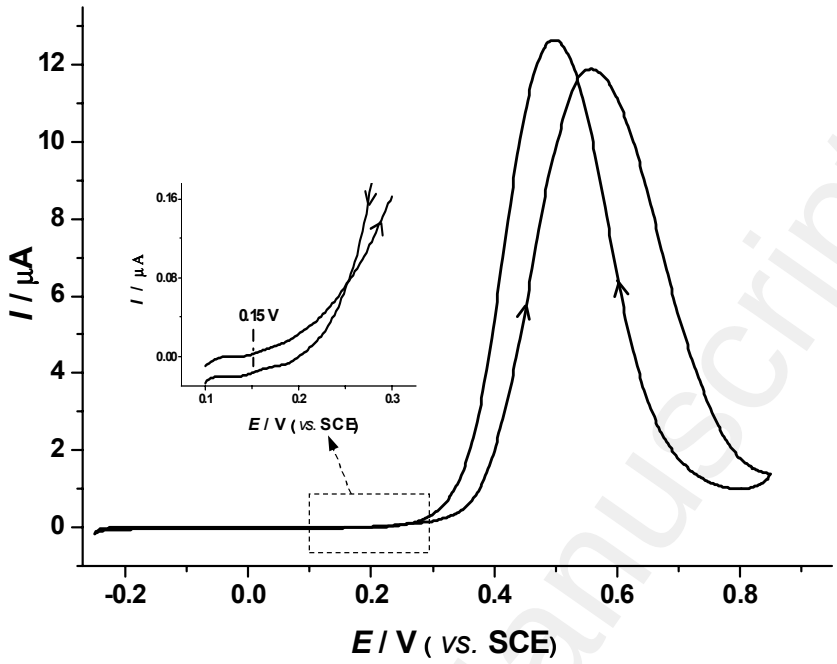

Fig.5 CVs of methanol oxidation on PtME(140) in 0.1 M CH_3OH +0.5 M H_2SO_4 solution, sweep rate 0.005 $V \cdot s^{-1}$.

Li, J. T.; Sun, S. G. et al., Fig. 5

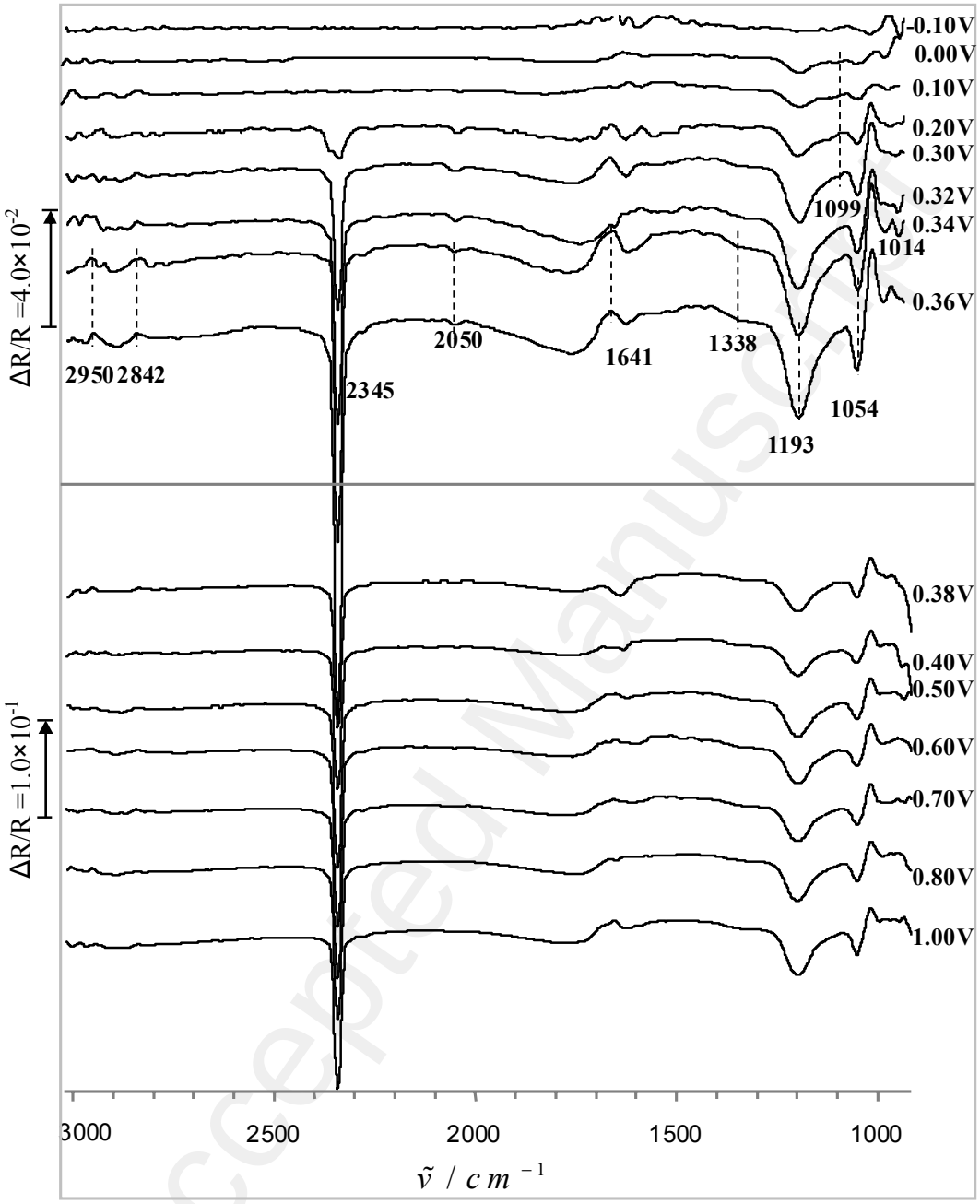

Fig. 6 In situ SPAFTIR spectra for methanol oxidation on PtME(140) in 0.1 M CH_3OH + 0.5 M H_2SO_4 solution, E_R = -0.20 V, E_S values are indicated in the spectra.

Li, J. T.; Sun, S. G. et al., Fig.6

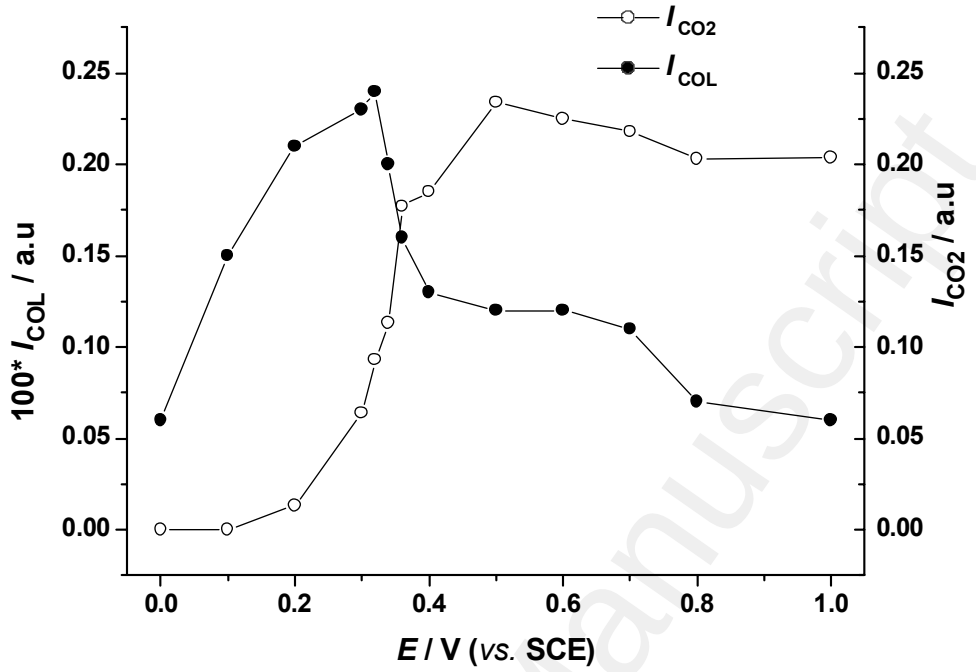

Fig. 7 Variation of I_{COL} and I_{CO2} with E_S, which obtained from the SPAFTIR spectra of methanol oxidation on PtME(140) in 0.1 M CH_3OH + 0.5 M H_2SO_4 solution.

Li, J. T.; Sun, S. G. et al., Fig. 7

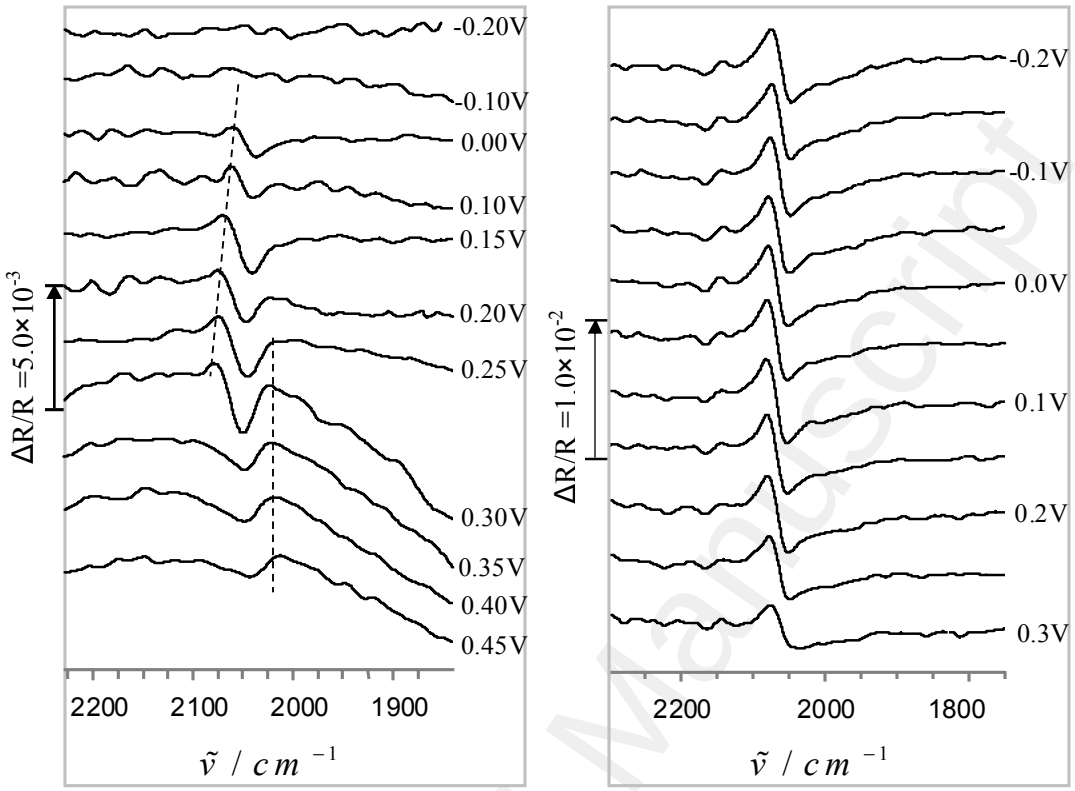

Fig. 8 (a) In situ SPAFTIR spectra of CO_L derived from CH_3OH on PtME(140) in 0.1 M CH_3OH + 0.5 M H_2SO_4 solution, E_R =-0.20 V. (b) In situ MSFTIR spectra of pre-saturated CO adsorbed on PtME(140) in 0.50 M H_2SO_4 solution saturated with CO, E_R= 0.80 V.

Li, J. T.; Sun, S. G. et al., Fig. 8

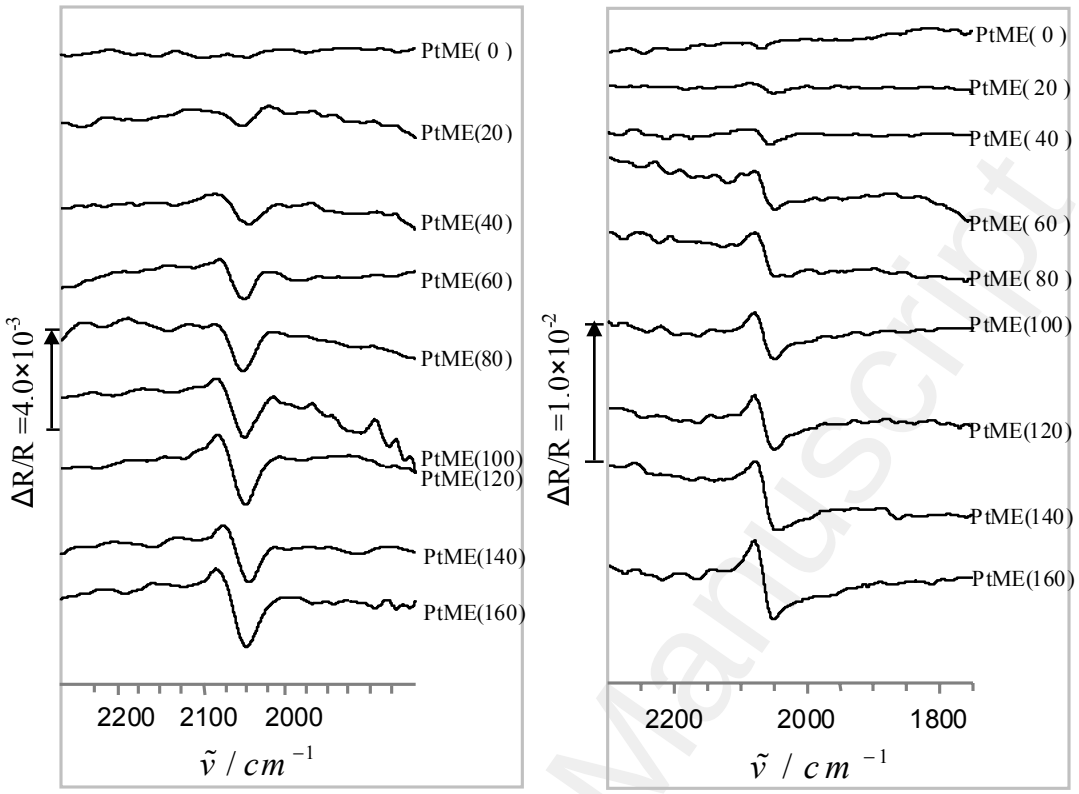

a b

Fig. 9 (a) In situ SPAFTIR spectra of CO_L derived from CH_3OH on PtME(*n*) in 0.1 M CH_3OH + 0.5 M H_2SO_4 solution. E_S = 0.20 V, E_R = -0.20 V. (b) In situ MSFTIR spectra for pre-saturated CO adsorbed on PtME(*n*) in 0.50 M H_2SO_4 saturated with CO. E_S = 0.2V, E_R = 0.80 V.

Li, J. T.; Sun, S. G. et al., Fig. 9

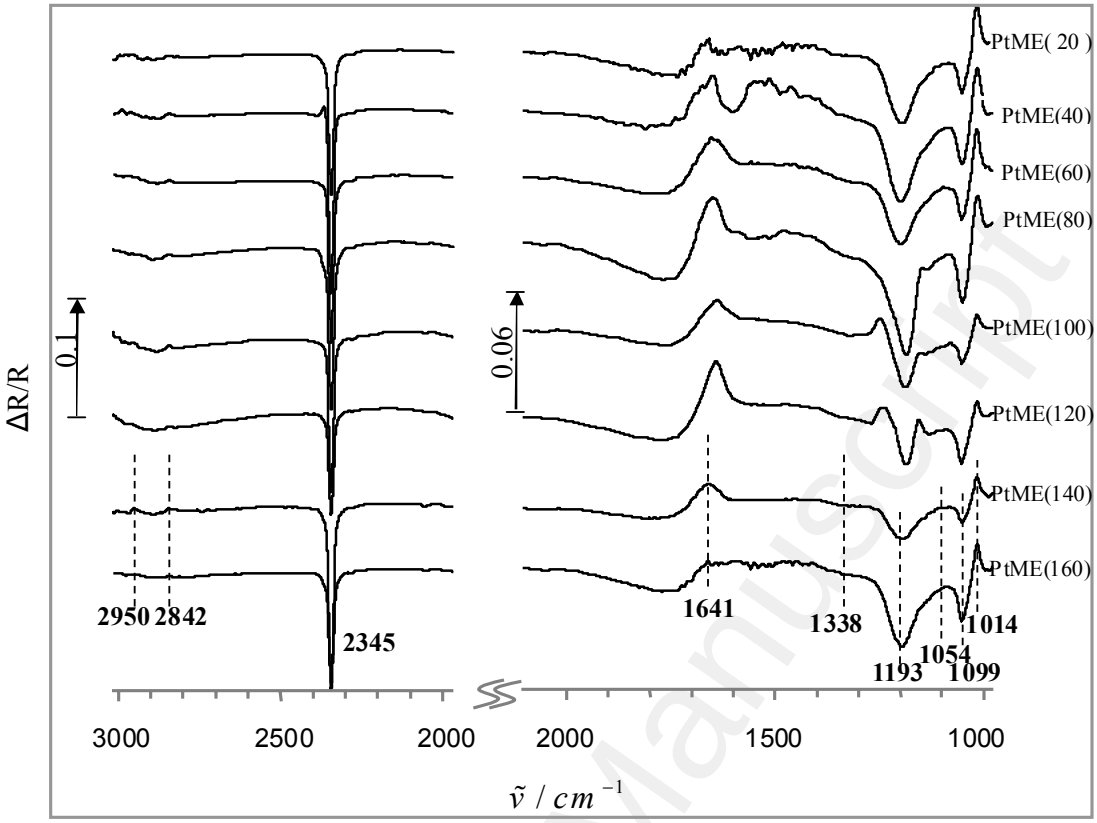

Fig. 10 In situ SPAFTIR spectra of methanol oxidation on PtME(n) in 0.1 M CH_3OH + 0.5 M H_2SO_4 solution, E_R = -0.20 V, E_S=0.4V.

Li, J. T.; Sun, S. G. et al., Fig.10

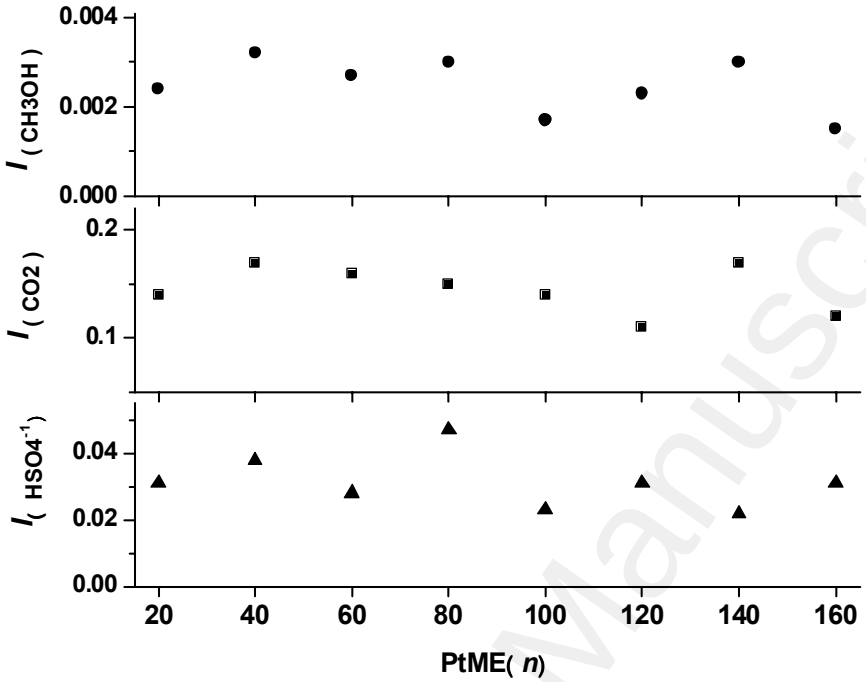

Fig. 11 Comparison of the intensity of CH_3OH band at 2842 cm^{-1}, CO_2 band at 2345 cm^{-1} and HSO_4^{1-} band at 1193 cm^{-1} PtME(n) at 0.40 V, obtained from the SPAFTIR spectra of methanol oxidation in 0.5 M H_2SO_4 + 0.1 M CH_3OH solution, E_R = -0.20 V.

Li, J. T.; Sun, S. G. et al., Fig.11

Table 1 Comparison of E_p and I_p of the cyclic voltammograms on the PtME(n) in 0.1 M CH_3OH + 0.5 M H_2SO_4 solution, sweep rate 0.005 $V \cdot s^{-1}$.

PtME(n)	0	20	40	60	80	100	120	140	160
E_P / V	0.571	0.549	0.551	0.555	0.557	0.555	0.558	0.557	0.557
I_P / μA	0.158	2.111	4.231	5.891	7.741	9.921	10.59	11.89	12.54

Table 2. List of I_{COL} derived from methanol on PtME(n) at 0.20 V, which obtained from SPAFTIR spectra of methanol oxidation in 0.1 M CH_3OH + 0.5 M H_2SO_4 solution, E_R = -0.20 V.

PtME(n)	0	20	40	60	80	100	120	140	160
I_{CO}*100	0.02	0.05	0.11	0.20	0.20	0.23	0.28	0.27	0.33